

Coupled solid and fluid mechanics simulation for estimating optimum injection pressure during reservoir CO₂-EOR

Ayub Elyasi^{1a}, Kamran Goshtasbi^{*1}, Hamid Hashemolhosseini^{2b} and Sharif Barati^{3c}

¹Department of Rock Mechanics, Tarbiat Modares University, Tehran, Iran

²Department of Mining Engineering, Isfahan University of Technology, Isfahan, Iran

³Faculty of mining, petroleum and geophysics, Shahrood University of technology, Shahrood, Iran

(Received November 30, 2015, Revised March 3, 2016, Accepted March 8, 2016)

Abstract. Reservoir geomechanics can play an important role in hydrocarbon recovery mechanism. In CO₂-EOR process, reservoir geomechanics analysis is concerned with the simultaneous study of fluid flow and the mechanical response of the reservoir under CO₂ injection. Accurate prediction of geomechanical effects during CO₂ injection will assist in modeling the Carbon dioxide recovery process and making a better design of process and production equipment. This paper deals with the implementation of a program (FORTRAN 90 interface code), which was developed to couple conventional reservoir (ECLIPSE) and geomechanical (ABAQUS) simulators, using a partial coupling algorithm. A geomechanics reservoir partially coupled approach is presented that allows to iteratively take the impact of geomechanics into account in the fluid flow calculations and therefore performs a better prediction of the process. The proposed approach is illustrated on a realistic field case. The reservoir geomechanics coupled models show that in the case of lower maximum bottom hole injection pressure, the cumulative oil production is more than other scenarios. Moreover at the high injection pressures, the production rates will not change with the injection bottom hole pressure variations. Also the FEM analysis of the reservoir showed that at CO₂ injection pressure of 11000 Psi the plastic strain has been occurred in the some parts of the reservoir and the related stress path show a critical behavior.

Keywords: geomechanics; coupled; bottom hole pressure; FEM; plastic strain; stress path

1. Introduction

Carbon dioxide (CO₂) sequestration is one of the most effective methods to reduce the amount of CO₂ in the atmosphere by injecting CO₂ into geological formations. There are some CO₂ sequestration projects (in progress or planned) around the world, e.g., Weyburn in Canada, In Salah in Algeria, Sleipner in Norway, Frio in USA, Qinshui Basin in China, Yubari in Japan, etc (Metz 2005). Furthermore, CO₂ sequestration could be combined with enhanced oil recovery

*Corresponding author, Associate Professor, E-mail: goshtasb@modares.ac.ir

^aPh.D. Student, E-mail: a.elyasi196@yahoo.com

^bAssociate Professor, E-mail: hamid@cc.iut.ac.ir

^cMSc Graduated, E-mail: sharifbarati@gmail.com

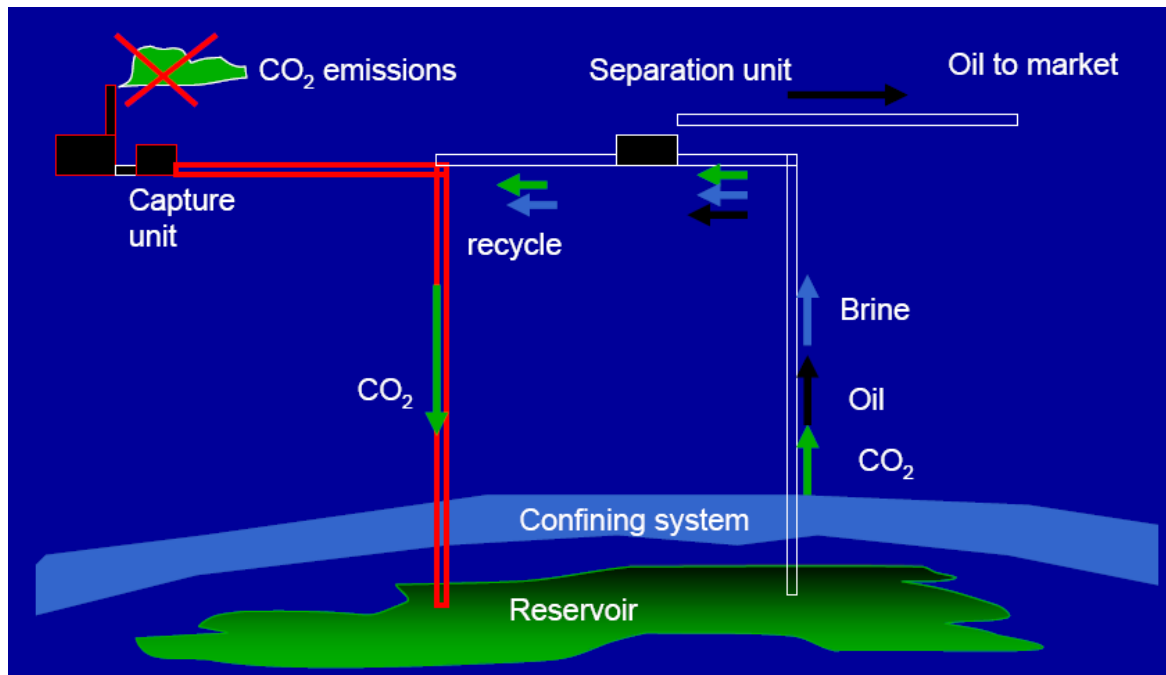


Fig. 1 Schematic of a CO₂-EOR system

(EOR) scheme (Jessen *et al.* 2005, Ravagnani *et al.* 2009, Carneiro 2009, Sbair and Azaroual 2010, Alavian and Whitson 2009, Blunt *et al.* 1993, Ferguson *et al.* 2010, Jahangiri and Zhang 2010). From some studies (Jahangiri and Zhang 2010, Holt *et al.* 2000, Martin and Taber 1992, Todd and Grand 1993, Holt *et al.* 1995), the CO₂-EOR scheme is able to increase the oil production by 7-23% of the original oil in place (OOIP). Hence, the CO₂-EOR scheme has double benefits i.e., improving the oil production while reducing the amount of CO₂ in the atmosphere at the same time.

In the reservoir, CO₂ moves outward away from the injection well in a generally radial manner by entering the brine and/or oil-filled intergranular or intercrystalline pores of a generally tabular body of sedimentary rock bounded by an upper confining system that greatly retards vertical movement of CO₂ (Fig. 1).

Storage of CO₂ in subsurface systems involves transmitting the fluid into the desired formation depth. The rate of injection should be such that will not offset the stability of the system; however, the introduction of fluid will lead to an increase in the formation pressure, which without proper injection pressure and control may result in mechanical failure of the material. As indicated in Bauer *et al.* (2012), Park *et al.* (2012), tracking pressure development as the CO₂ is being injected and during post-mortem periods is essential in ensuring safety limits are not exceeded. Therefore geomechanical modeling plays a very important role in risk assessment of geological storage of CO₂.

Petroleum geomechanics has become more-and-more part of oil industry analysis approaches to explain and evaluate phenomena such as wellbore stability in shale, reservoir compaction and surface subsidence during depletion, injection, hydraulic fracture stimulation, and so on (Fjaer 1992, Zhou *et al.* 1996, Chales and Roatesi 1999, Kaarstad and Aadnoy 2005, Dusseault 2011,

Elyasi *et al.* 2014, Goshtasbi *et al.* 2014, Elyasi and Goshtasbi 2015). Also reservoir simulation is growing rapidly in the recent decades. Modeling and simulation of reservoir is very useful in predicting the performance of the reservoir. Application of reservoir simulation in CO₂ sequestration has been developed in the recent years. Many people have done the modeling and simulation of CO₂ injection in the reservoir (Sbai and Azaroual 2010, Alavian and Whitson 2009, Bielinski 2007, Hayek *et al.* 2009, Nasrabadi *et al.* 2009, Sun and Firoozabadi 2009, Thomas and Wheeler 2011, Sifuentes *et al.* 2009, Moortgat *et al.* 2010, Izgec *et al.* 2005, Nghiem *et al.* 2010, Liu *et al.* 2010, Kumar *et al.* 2004, Oldenburg 2001, Eigestad *et al.* 2009).

During CO₂ sequestration different physical processes that involve multiphase and multi-component fluid flow in a geologic system take place. In order to study the mechanical deformations during CO₂ sequestration, numerical modeling of fluid flow through porous medium coupled with a geomechanical analysis of the medium at different pore pressure distributions (Rutqvist *et al.* 2002, Settari and Mourits 1998, Settari and Walters 1999, Thomas *et al.* 2003, Vidal-Gilbert *et al.* 2009) is required. This coupling can be achieved either by a fully or partially coupled numerical simulation.

There are a number of methods that might be used to couple together fluid flow and geomechanical simulation, including full coupling, one-way coupling, explicit coupling and iterative coupling (Dean *et al.* 2003). The fully coupled method involves solving the equations for fluid-flow and geomechanical deformation simultaneously in the same simulator. This is the most accurate numerical method. However, it is difficult to implement, and no commercial simulators with this facility currently exist. As a result, simplifications would have to be made in the fluid and geomechanical equations.

The other three methods all use separate fluid-flow and geomechanical simulators, meaning that commercial finite element fluid-flow and geomechanical deformation codes can be used. The simplest method is one-way coupling, where the pore pressure and fluid properties computed by the flow simulator are passed to the geomechanical simulation at user-defined timesteps. The results of the geomechanical simulation are not passed back to the fluid flow simulation. As a result, this method will only be appropriate where deformation is not large enough to significantly affect porosity and permeability.

For the explicit coupling method, the fluid flow simulator is again run until a user-defined time step, where the pore pressure is passed to the geomechanical simulation. However, unlike the one-way coupling method, the changes in porosity and permeability are returned to the fluid flow simulator for use in subsequent time steps. As a result, the explicit method is more accurate than the one-way method, but as it requires the passing of data in two directions, is more computationally expensive (Dean *et al.* 2003). The iterative method is similar to the explicit method; except for at each time step the fluid flow and deformation are solved in an iterative manner, with data passed back and forth between the simulations until a stable solution is found.

We report here the development of an explicit coupled multiphase flow and geomechanical approach to analyze HM coupled processes relate to CO₂ injection into oil reservoir. The explicit coupled study utilizes a reservoir model for simulation of fluid flow through porous media using the commercial fluid flow simulator ECLIPSE 300 (Schlumberger 2010) and the optimized finite element discretization using the commercial finite element solver ABAQUS (Dassault Systemes 2010) for the geomechanical analysis of rock deformation that is caused by the pore pressure difference associated to enhanced oil recovery using carbon dioxide (CO₂-EOR). A case study with different scenarios has been examined to illustrate the method and impact of these coupled processes. Finally, we conclude with a discussion on the obtained results.

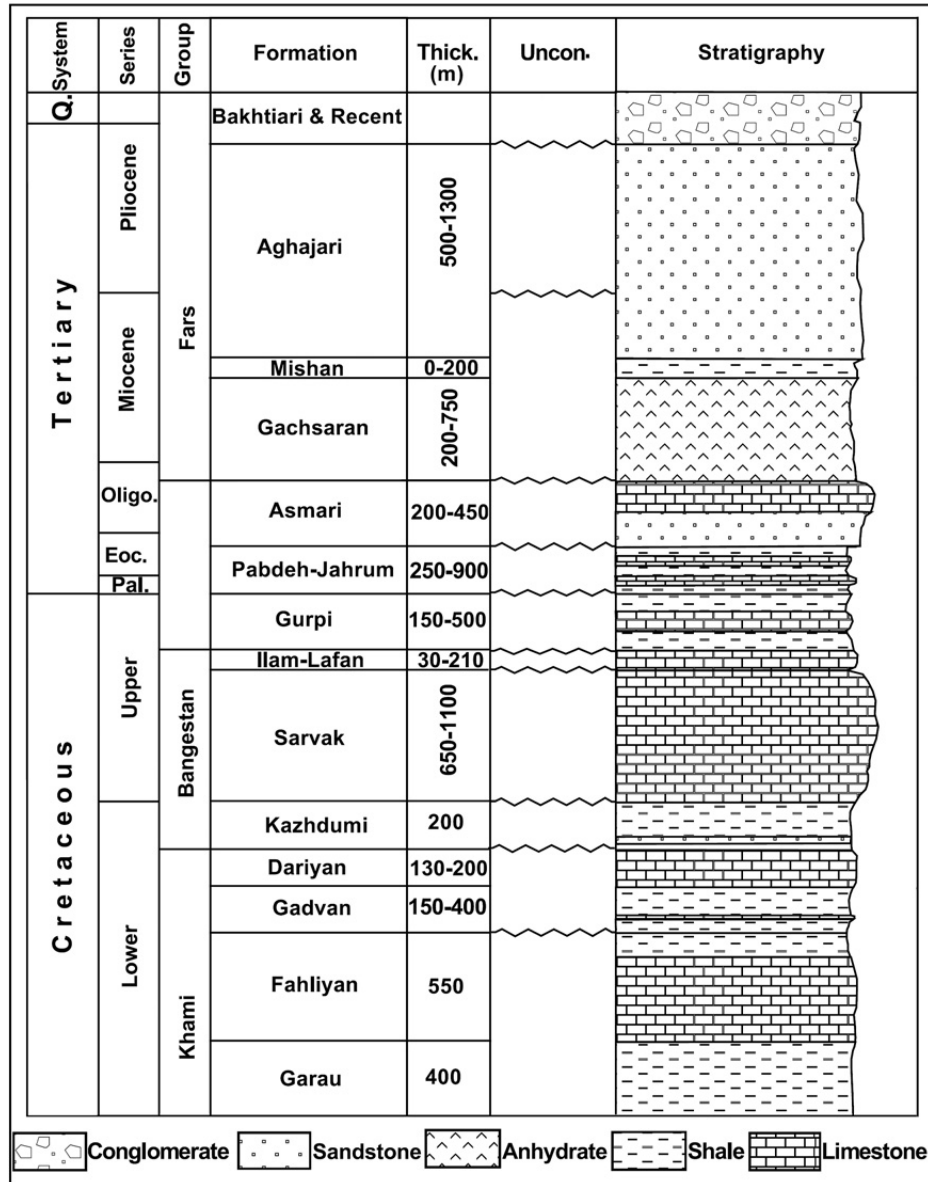


Fig. 2 Sequence Stratigraphy of the studied region (Alavi 2004)

2. Site description

The studied oil region is located in south west of Iran. The region has little folding, with numerous reservoirs. Sequence stratigraphy of the region, respectively, from top to the target depth includes Aghajari, Gachsaran, Asemari, Pabdeh, Gurpi, Ilam, Lafan, Sarvak, Kazhdumi, Darlyan, Gadvan, Fahliyan and Garau.

In this study the Sarvak formation was the target reservoir. This reservoir is an anticline structure directed to north-south with no exposure and it was detected by geophysical (seismic)

survey. No major faults and fractures have been reported in this reservoir.

The Sarvak formation (Cretaceous, thick 650-1100 m) is a thick carbonated unit that was deposited in 'Neotethys southern margin of Zagros area. It is one of the most important hydrocarbon horizons in Iran. Laboratory and field observation lead to recognition of four facies environments: open marine, shale, and lagoon in coastal area of Fars, Khuzestan and Lurestan. The lower lithostratigraphic limit of Sarvak Formation, which is conformable and gradational, overlies the Kazhdumi Formation. Upper lithostratigraphic limit of that is secant with Ilam-Lafan Formation (Fig. 2). Also thickness and layers slope of Sarvak formation is approximately constant.

The reservoir depth is about 2700 m and has a thickness of approximately 110 meters. Limestone is the dominant rock type in this reservoir and also upper structure. The reservoir geometry has been indicated by five wells drilled in the structure and the information related to the distance between the wells and connection depth of them to Sarvak formation.

The reservoir upper surface was sketched by introducing the intersection points from wells and the formation in Surfer software (Fig. 3). Finally, the reservoir geometry was determined by its upper surface and the thickness of layers.

The mechanical properties and initial stress profile is required to be added to the geomechanical model and coupled with the flow model in order to be able to study the mutual effect of pressure and stresses and the resulting effect on integrity and injectivity. The reservoir rock mechanical parameters including, uniaxial compressive strength, young modulus and poisson ratio were obtained from Dipole sonic imager (DSI) logs, laboratory tests and empirical relationships.

The reservoir young modulus and poisson ratio can be obtained by

$$\vartheta = \frac{v_p^2 - 2v_s^2}{2(v_p^2 - v_s^2)} \quad (1)$$

$$E_{\text{dyn}} = 2G(1 + \vartheta) \quad (2)$$

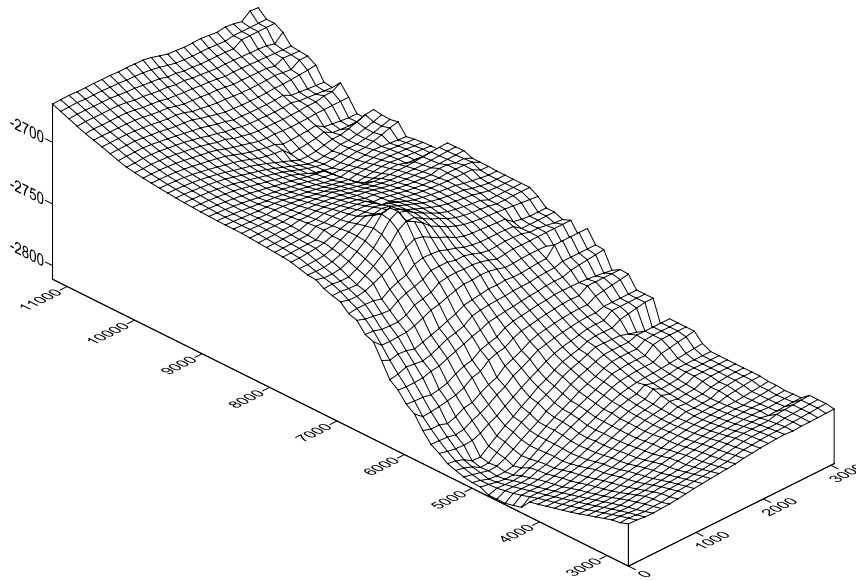


Fig. 3 The reservoir upper surface

Table 1 Mechanical properties of the reservoir layers

Layer	Thickness (m)	Water saturation (%)	Porosity	Permeability (md)	Density (Kg/m ³)
1	5	90	0.01	2	2600
2	20	15	0.1	40	2600
3	30	20	0.14	40	2600
4	60	45	0.1	40	2600
5	5	90	0.01	2	2600

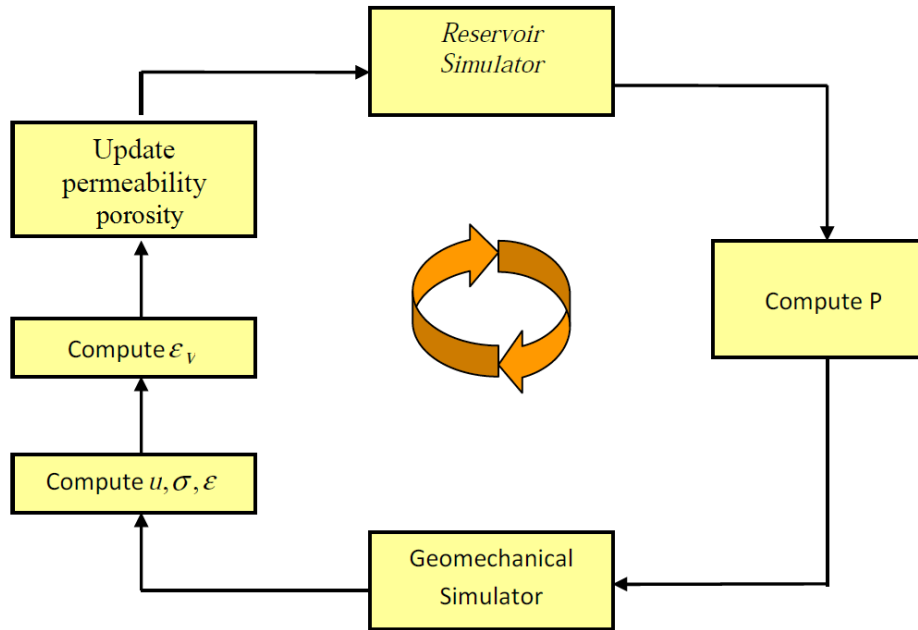


Fig. 4 Coupled system flowchart

$$E_{static} = 0.4E_{dyn} \quad (3)$$

Where ν is poisson ratio. v_s and v_p are shear and compression sonic velocity respectively. Also E_{dyn} is dynamic young modulus and E_{static} is static young modulus.

The reservoir young modulus, poisson ratio, cohesion, friction angle and uniaxial compressive strength are 25 GPa, 0.20, 3.5 MPa, 32 and 60 MPa respectively.

Densities of water, oil and gas are 1190, 850 and 0.90 Kg/m³ respectively. Also the reservoir initial pressure is around 4100 psi. Other characteristics of the reservoir layers are given in Table 1.

3. Reservoir-geomechanics coupling

3.1 Approach

The explicit coupling approach consists in executing sequentially the two models, linked

through external coupling modules (Fig. 4). The fluid flow simulator is executed first over a first period. Updated pore pressures at the end of this first period are interpolated and transferred into the geomechanics grid in the geomechanical simulator.

Based on the updated producing conditions and constitutive relationships, the geomechanical simulator calculates the strains. Then the reservoir permeability and porosity are modified according to theoretical or empirical functions (between volumetric strain, permeability and porosity). Updated grid block permeabilities and porosities are then transferred to the fluid flow simulator for the execution of the next time period.

A simple and empirical relationship is proposed by Touhidi-Baghini (1998) for predicting the evolution of the absolute permeability changes induced by stress changes. This simple relationship linking permeability changes to volumetric strain reads

$$\ln \frac{k_1}{k_0} = \frac{c}{\phi_0} \varepsilon_v \quad (4)$$

This equation allows the computation of absolute permeability k_1 from its initial value k_0 , the volumetric strain ε_v and the initial porosity value (ϕ_0). An appropriate value for the constant c has to be picked. According to Touhidi-Baghini (1998), the values $c=5$ and $c=2$ appear to be appropriate to match with vertical and horizontal permeability evolutions, respectively.

The porosity (ϕ), is related to the volumetric strain as (Zienkiewicz *et al.* 1999)

$$\phi = \phi_0 + \alpha(\varepsilon_v - \varepsilon_{v0}) + \frac{1}{\varphi}(P - P_0) \quad (5)$$

Where α and φ are constant parameters (Biot 1940). The amount of α and φ for the studied reservoir are one and infinite respectively. Also P_0 is initial reservoir pore pressure and ε_{v0} is initial volumetric strain.

3.2 Reservoir modeling

The results of the standard reservoir studies carried out for the management of the field production provide part of the inputs necessary for a geomechanical finite element analysis. The typical workflow of a reservoir study consists of a “static” study and a “dynamic” study.

A static reservoir study typically involves four main stages including Structural modelling, Stratigraphic modelling, Lithological modelling and Petrophysical modelling. That means the “static” model includes the detailed reconstruction of the geological structure of the reservoir (e.g., the shape of the layers and the trend of the faults), the definition of the mineralized volumes and the attribution of the petrophysical parameters (initial porosity and permeability) as a function of the location. The “dynamic” model is built with the flow simulator (ECLIPSE 300). The dynamic model takes as input all the information of the static model and, by introducing a series of additional parameters regarding the characteristics of the fluids, the rock and the well system, provides the information required for the field management, such as the dynamic reserve evaluation injection and the production profiles as a function of the development scenarios. As an example, in Fig. 5 the finite difference discretization of a dynamic model for the oil field is shown.

The dynamic model provides as output sets of data that are used in the geomechanical finite element simulation: the grid discretization of the reservoir and of the surrounding areas; the initial values of porosity and permeability; the evolution of the fluid pressure as a function of space and time. As explained in detail in the following section, all these information are converted with an interface code and used to build the ABAQUS FE model.

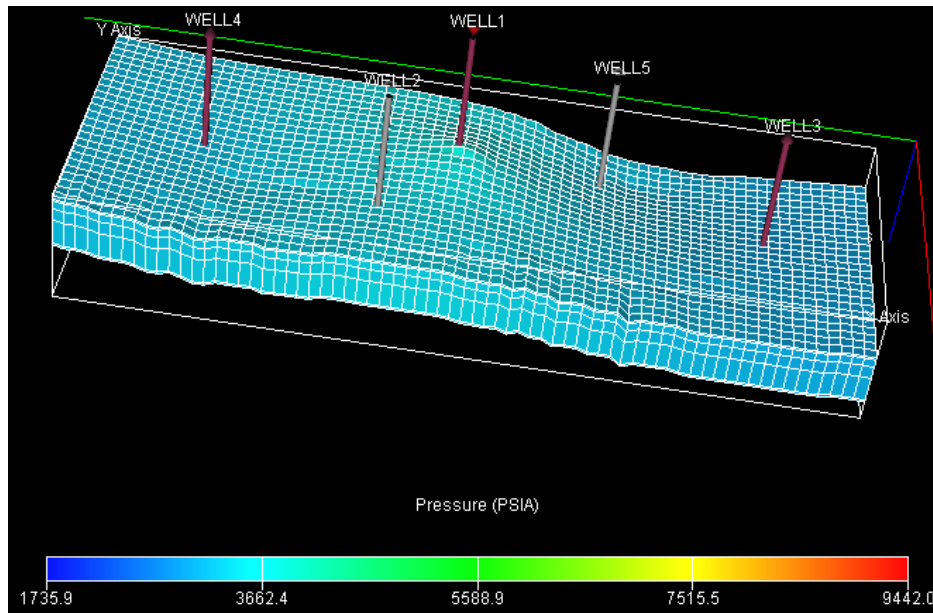


Fig. 5 Flow model: grid discretization, well system and pressure distribution at 25 Sep 2015

3.3 Geomechanical modeling

To model a reservoir-geomechanics coupled simulation, irrespective of the used gridding technique, three apparent choices exist regarding establishing the geomechanical model and reservoir model:

1. Modeling just the reservoir part in geomechanical simulator and reservoir simulator (Fig. 6(a))
2. Construction of reservoir part in reservoir simulator, and reservoir surrounded by rocks in geomechanical simulator (Fig. 6(b)).
3. Modeling the reservoir part and the surrounding strata (here, overburden and underburden) in both simulators (Fig. 6(c)).

Examples of these approaches may also be found in many articles (Lerat *et al.* 2009, Shi and Durucan 2009, Zandi *et al.* 2010).

The weakness of the first approach is the setting of an equilibrium state in the geostatic step of the geomechanical simulation.

The second approach is the most commonly used, as we aim at a limited total number of elements in the models in order to reduce the simulation run time.

In the third approach, the reservoir surrounded by rocks is constructed in both simulators, which can result in increase of the simulation run time. Using an adapted reservoir simulator, the advantage of this method is the possibility of correctly simulating the temperature field in surrounding rocks.

In current paper, because of studding only HM coupling, the second approach has been used for establishing the geomechanical model and reservoir model.

The fact that the grid type in reservoir simulator is different from geomechanical simulator makes the mapping process more complicated. In fact in the reservoir simulator a finite difference

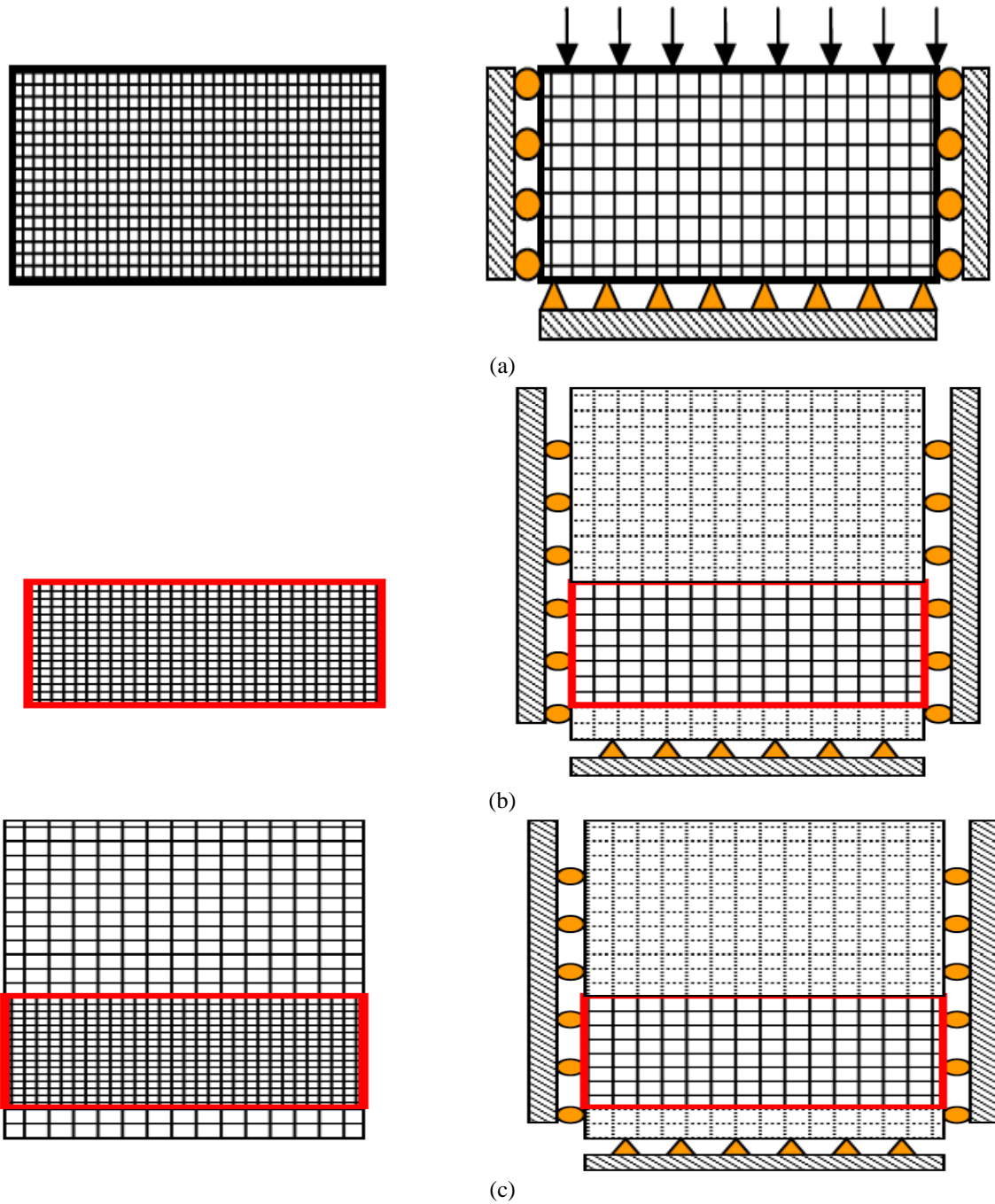


Fig. 6 Different 2D geometries of modeled reservoir in reservoir simulator (left) and its surrounding rocks in geomechanical simulator (right)

discretization is used where flow variables are computed at the center of grid blocks while in the geomechanical simulator a finite element grid discretization is used to compute displacements at

the nodes of the grid.

If the grids in reservoir simulator and geomechanical simulator are coincident, interpolation of the data between the two simulators is simple. Updated pore pressures computed in the center of reservoir grids, at the end of this first period, are transferred on the nodes of geomechanics grids in geomechanical simulator. In this transfer, data are interpolated to pass from finite difference discretization to finite element discretization and inversely.

In geomechanical reservoir simulation the reservoir zones (not external boundary) must be refined (to obtain realistic results), so the grids in reservoir and geomechanical simulators are not coincident and passing the data (pressure, volumetric strain and etc.) between the two simulators is more complex. In this case a field transfer algorithm must be used to perform the passing of data from a grid to the other. Here a develop of FORTRAN 90 interface code is used for mapping the data from reservoir grid centers to geomechanics grid nodes and vice versa.

The geometrical information of the ECLIPSE 3D corner point grid are directly extracted from the relevant output files of the flow model and processed to build the FE mesh in the reservoir region. This approach allows for the definition of a FE model which is fully consistent with the reservoir FD model.

The typical FD and FE grid structures are shown in Fig. 7 for a 2D mesh.

The external part (side-burden, over-burden and under-burden) of the grid, needed to correctly simulate the geomechanical behavior of the system, is automatically built by the interface code, provided that the final model size is given. The element type attributed to the reservoir regions is 8-node brick stress/displacement/pore pressure (C3D8P), while 8-node brick stress/displacement (C3D8) is assigned to the external regions.

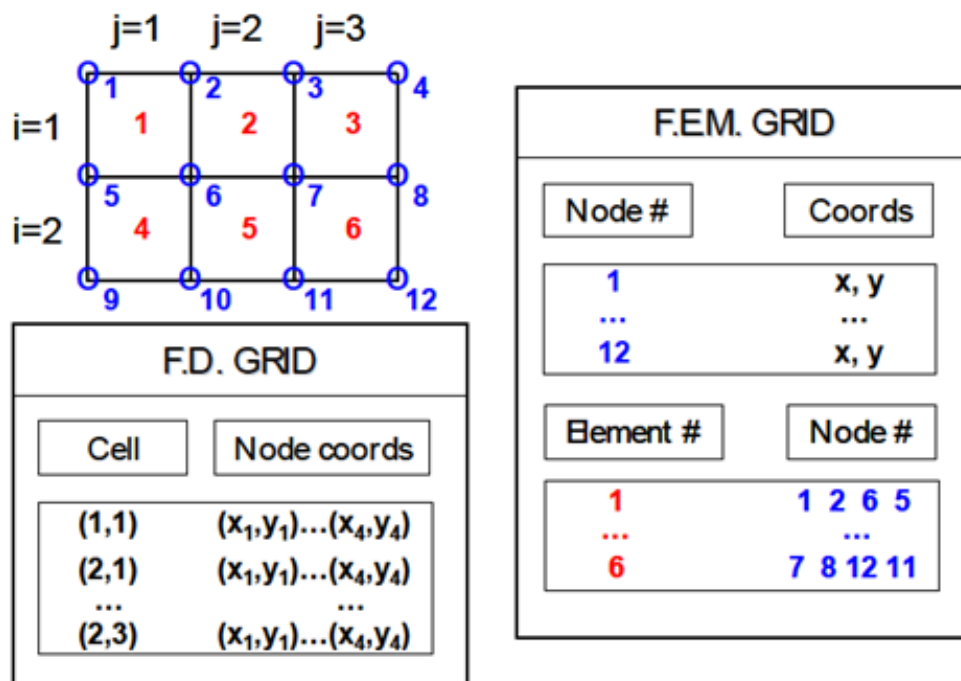


Fig. 7 From FD to FE grid

3.4 Prescribed conditions

The initial effective stresses are generated in the ABAQUS subroutine, SIGINI.

The initial geostatic stress field must be in equilibrium with the applied loads and boundary conditions. Ideally, the loads and initial stresses should exactly equilibrate and produce zero deformations. This state is obtained performing an initial ABAQUS analysis fixing all displacements degree of freedoms. Calculated reaction forces written to the ABAQUS output file are then used to create nodal point forces, which are applied in the first step of the actual ABAQUS analysis.

The pore pressure depletion and injection history within the reservoir is transferred from the ECLIPSE reservoir model to ABAQUS utilizing the user subroutine DISP. A file containing the pore pressure in each ECLIPSE block is read for each time step analyzed by ABAQUS.

The initial porosity distribution is transferred from the ECLIPSE reservoir model to ABAQUS utilizing the user subroutine VOIDRI for reading initial porosity in ABAQUS. The initial void ratio e_0 , defined as the ratio between the pore volume and the solid volume, is related to the porosity n through: $e_0 = n / (1 - n)$.

The boundary condition for the fluid flow model is that there is no flow across the boundary of the model. The constraints for the geomechanical model are as follows. The right, left, front and back sides of the model are fixed in the x -direction and y -direction so there would be no displacement in the x and y directions. The bottom side of the model is fixed in all directions and the top of the model is free to move in all directions.

4. Results and discussion

As shown in Fig. 5, the reservoir was targeted by five wells. Production conditions and restrictions are as follow:

- Oil production rate of each well is 3,500 stb/day (standard barrels per day) and the minimum bottom hole pressure is 1450 Psi.
- Oil production of each well will be terminated if the well production rate is less than 500 stb/day or GOR (reservoir gas and CO₂ oil ratio) is greater than 20 mscf/stb (thousand standard cubic feet per stock tank barrel).

Also production and injection strategies are as:

Oil production of all wells started at January 1th 1997. If any of the wells production was terminated (because of mentioned restrictions) the well will be used as a CO₂ injection well. Injection strategy involves the injection of 200 mmscf/day (million standard cubic feet per day) and four scenarios for the maximum bottom hole pressure were investigated as follow:

- 1- 5000 Psi (scenario 1)
2. 7000 Psi (scenario 2)
- 3- 9000 Psi (scenario 3)
- 4- 11000 Psi (scenario 4)

The reservoir production rate is shown in Fig. 8. As can be seen, at the beginning, each well production rate is 3,500 stb/day. Because of reservoir pressure reduction, the oil production rate will be decreased gradually. After about 3410 days from the start of production the production rate of well No.1 falls under 500 stb/day, so its production will be halted and it will be prepared for

Table 2 The wells production termination time and termination reasons at each injection scenario

scenario	Well No.1		Well No.2		Well No.5		Well No.4		Well No.3	
	day	reason	day	reason	day	reason	day	reason	day	reason
1	3410	OPR<limit*	6002	OPR<limit	6712	OPR<limit	15052	OPR<limit	18563	OPR<limit
2	3410	OPR<limit	6002	OPR<limit	6712	OPR<limit	12142	GOR>20* mscf/stb	14342	GOR>20 mscf/stb
3	3410	OPR<limit	6002	OPR<limit	6712	OPR<limit	11602	GOR>20 mscf/stb	12682	GOR>20 mscf/stb
4	3410	OPR<limit	6002	OPR<limit	6712	OPR<limit	11602	GOR>20 mscf/stb	12682	GOR>20 mscf/stb

*OPR<limit: the well oil production rate is less than 500 stb/day

*GOR>20 mscf/stb: the well gas phase (reservoir gas + CO₂) oil ratio is greater than 20 mscf/stb.

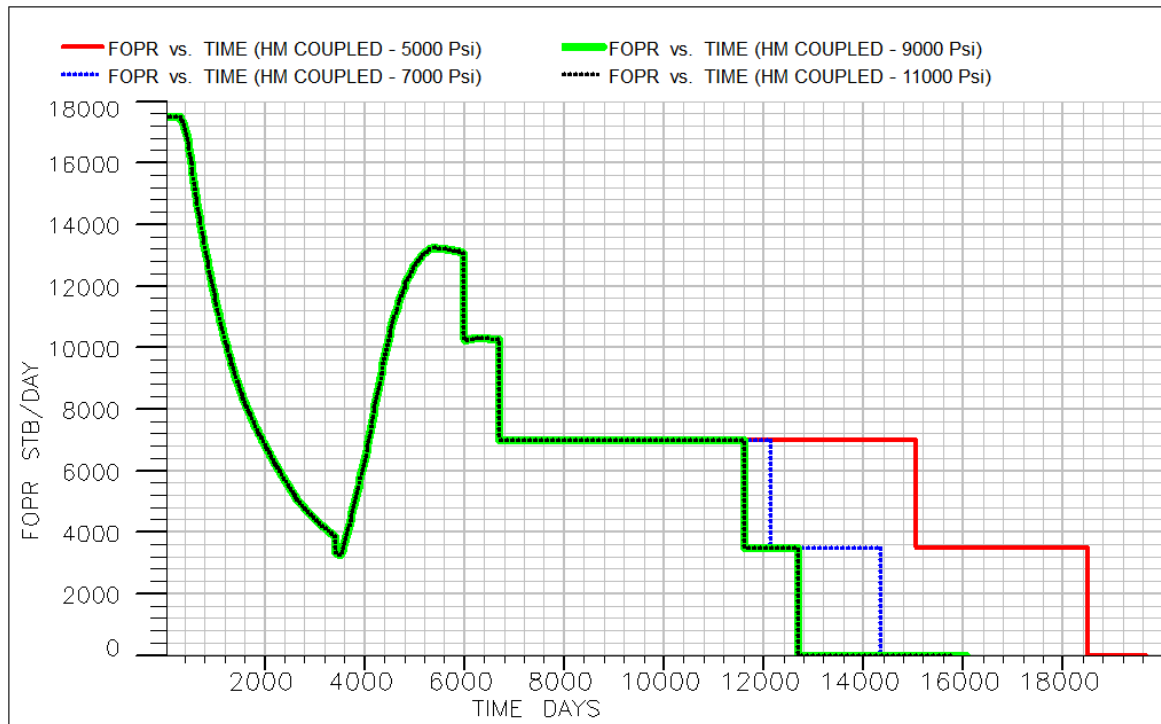


Fig. 8 reservoir oil production rate

CO₂ injection rate of 200 mmscf/day with four mentioned maximum bottom hole pressure scenarios.

At each of the scenarios, after CO₂ injection the reservoir pressure gradually increased and so the rate of production in four other production wells will increase.

Over the time of the reservoir injection and production, oil production from the wells will be halted at different times because of low production rate or GOR>20 mscf/stb. For all injection scenarios, the wells production termination time and reasons for this event are listed in Table 2.

The reservoir cumulative oil production for each of the scenarios is listed in Table 3.

Table 3 Cumulative oil production for each of the scenarios

Scenario	1	2	3	4
Cumulative production(stb)	1.35181e+008	1.10322e+008	1.02622e+008	1.02622e+008

Table 4 Cumulative CO₂ injection for each of the scenarios

Scenario	1	2	3	4
Cumulative CO ₂ injection(mscf)	2.03923e+009	1.79514e+009	1.96091e+009	2.30266e+009

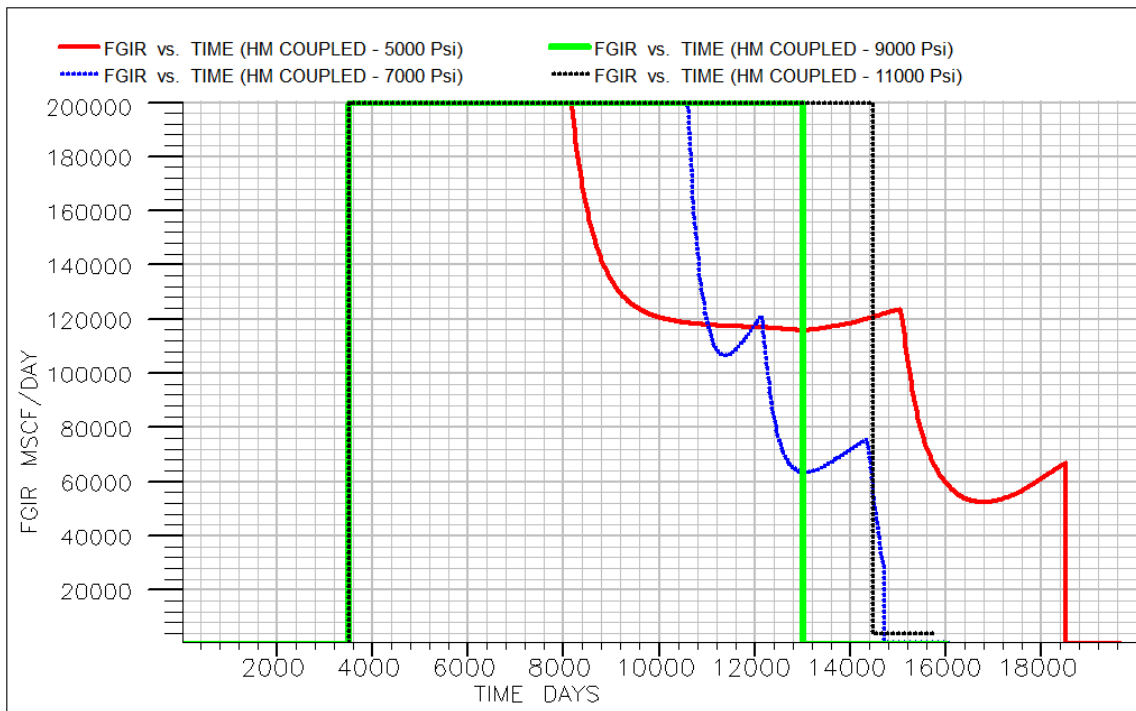


Fig. 9 well No. 1 gas (CO₂) injection rate

According to Table 3, In the case of lower maximum bottom hole injection pressure, the cumulative oil production is more than other scenarios. Moreover at the high injection pressures, the production rates will not change with the injection bottom hole pressure variations. So in this reservoir, CO₂ injection with a maximum bottom hole pressure of 5000 Psi is suggested in order to increase oil production.

After the reservoir production termination (the production wells termination), the CO₂ injection from well No. 1 will be continued in order to CO₂ sequestration in the depleted reservoir and removal pollutants from the environment. The reservoir cumulative CO₂ injection for each of the scenarios is listed in Table 4.

Since the lifetime of the reservoir in scenario 1 is greater than both scenarios 2 and 3, the cumulative injection of carbon dioxide in scenario 1 is also more than the other two scenarios. But in scenario 4 because of more bottom-hole pressure, the cumulative CO₂ injection is more than three other scenarios. The reservoir CO₂ injection rate for well No. 1 is shown in Fig. 9.

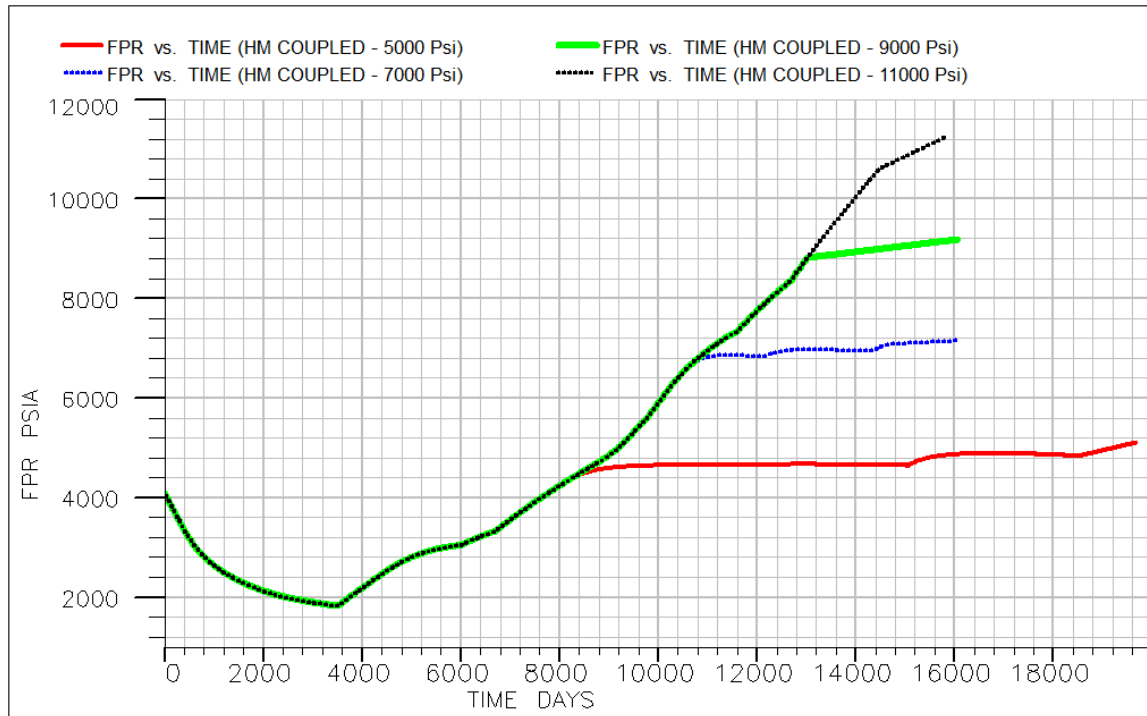


Fig. 10 reservoir pressure rate

Table 5 CO₂ injection termination time for each of the scenarios

Scenario	1	2	3	4
Termination time(day)	20330	15791	14111	15511

Due to the difference between the reservoir pressure and pressure at the bottom of injection well, CO₂ flow path is from bottom of the injection well to around it. At each of the scenarios, rate of reservoir pressure change is shown in Fig. 10. As can be observed, in spite of production from the four wells (No. 2, 3, 4 and 5) by increasing the time of gas injection from the well No. 1, the reservoir pressure gradually increases and by reduction of difference between the reservoir pressure and injection pressure the gas injection rate decreases. Therefore the slope of the reservoir pressure rate variations decreases until the injection will be stopped. The injection well (well No. 1) termination time for each of the scenarios are listed in Table 5.

The in-situ stress regime for the case study is NF stress regime with stress ratio (k) of 0.41 and Mohr-Coulomb elasto-plastic criterion was used for geomechanical simulation of the reservoir during CO₂-EOR. Also for studying the surrounding rocks the elastic model was used.

The change in porosity and permeability due to the change in pore pressure and the state of stress is reflected in the analysis by updating of corresponding parameters. The coupling module treats permeability as a non-linear function of stresses and is capable of detecting plastic deformation.

In the case of hydro-mechanical (HM) modeling, with the increase in pore pressure the reservoir permeability and porosity values has increased and also both decrease by pore pressure

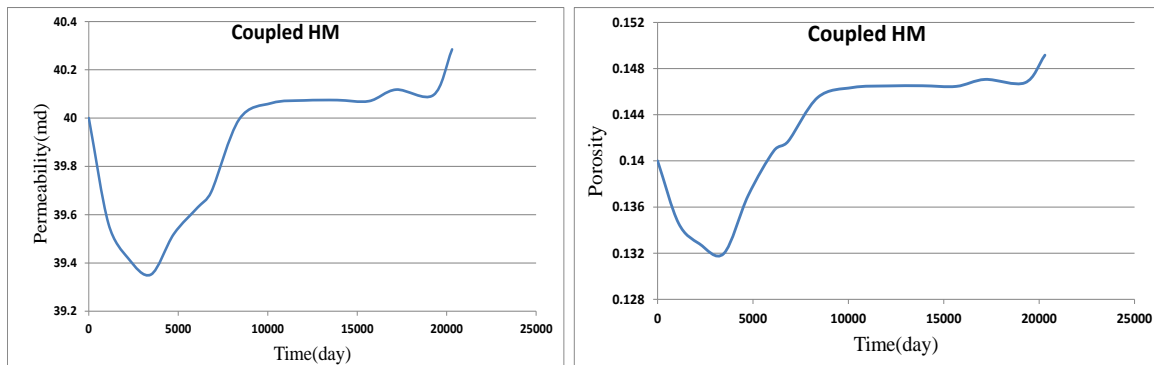
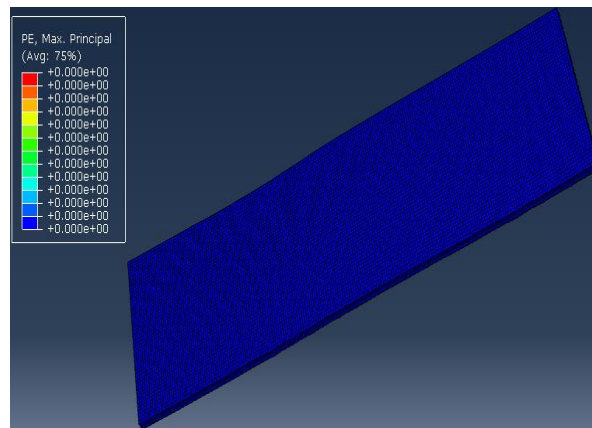
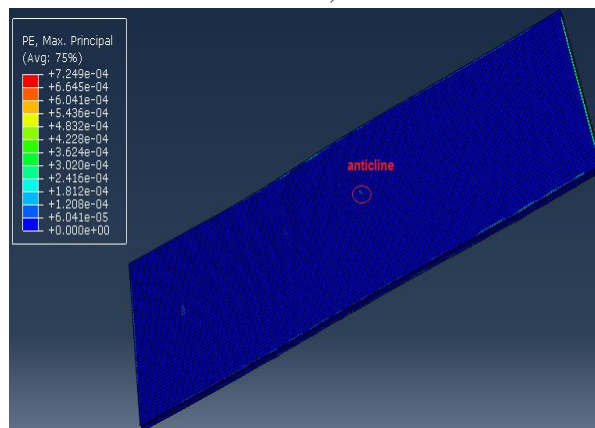


Fig. 11 Permeability (left) and porosity (right) changes around the injection well (zone No. 2677) with HM coupling



scenario 1, 2 and 3



scenario 4

Fig. 12 Maximum plastic strain in the reservoir

reduction (Fig. 11). Note that the changes in permeability and porosity are low because of a rather insensitive stress-permeability relationship for the porous reservoir rock.

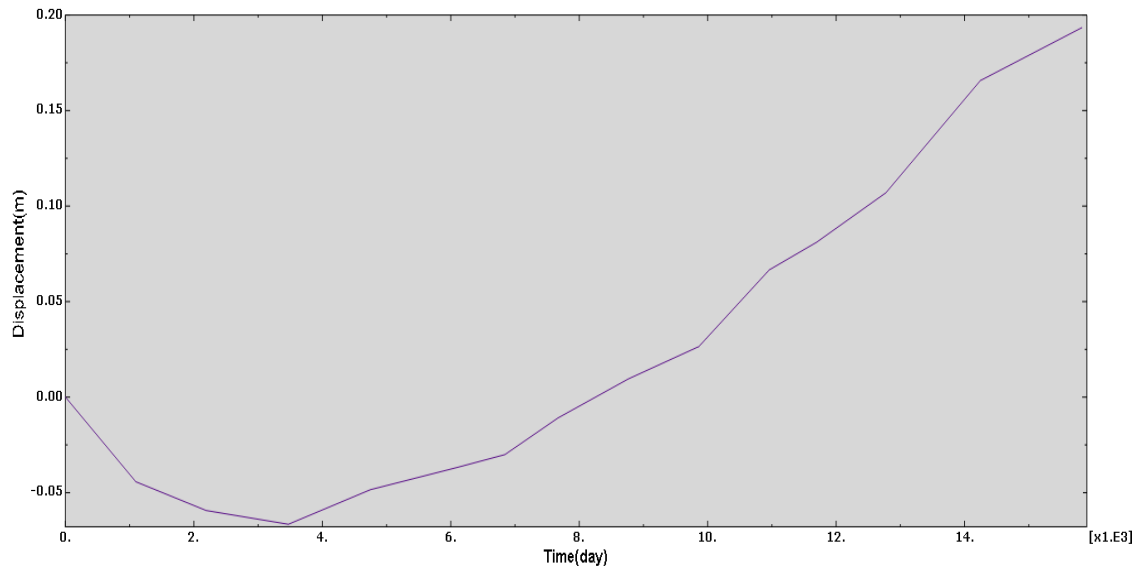


Fig. 13 Vertical displacement changes around the well No. 1 during production and injection for scenario 4

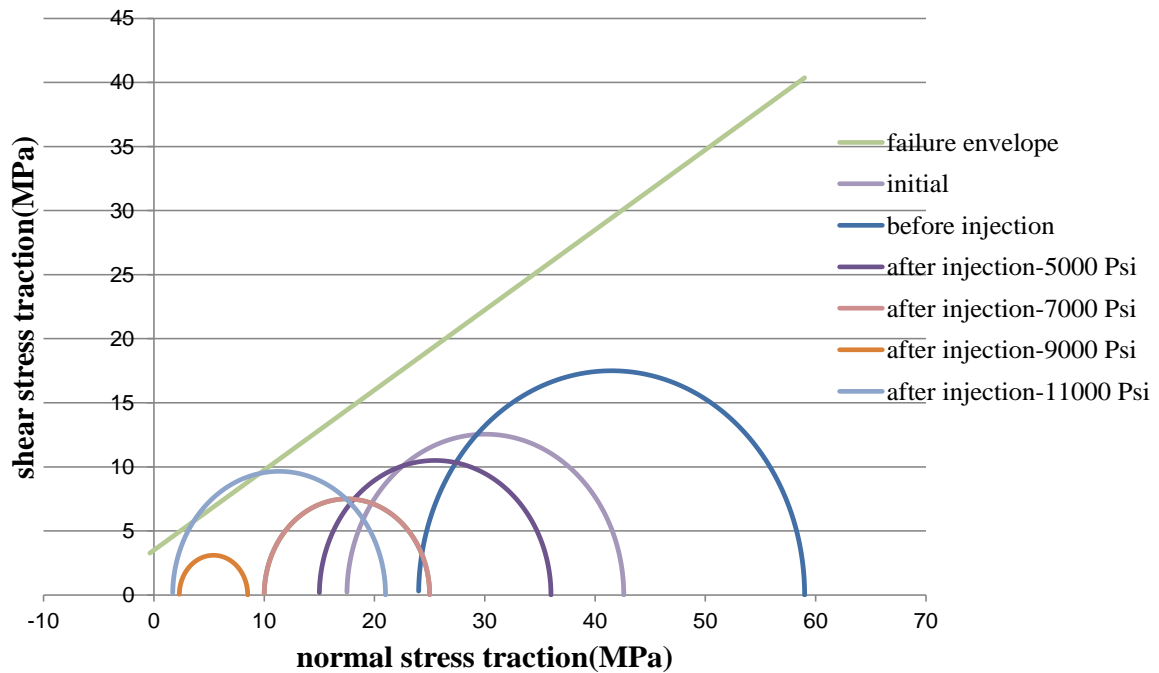


Fig. 14 Stress path for the reservoir for production and injection scenarios

The finite element analysis of the reservoir showed no sign of plastic strain under production and gas injection phases of scenario 1, 2 and 3 in any part of the reservoir but in scenario 4 (11000 Psi) plastic strain has occurred in some parts of the reservoir like the anticline part and side burdens (Fig. 12). During depletion and before the injection scenario of well No. 1, the reservoir

has shown subsidence. However by injection of well No. 1 and production from other four wells, at the same time, the reservoir displacement reversed (as an example, the vertical displacement changes for scenario 4 is shown in Fig. 13). Though, unlike scenario 4 that has a critical displacement (about 19 cm), in scenario 1 and 2 the displacements are ignorable (less than 1 cm and about 6 cm respectively) because of less potential for instability of the reservoir. Also the displacement of scenario 3 is approximately high (about 9 cm), but the reservoir instability hasn't occurred.

The geomechanical analysis of the reservoir showed that the uplift is somewhat restricted by the overburden stiffness as the reservoir maximum vertical displacement is about 6 cm at the top of the injection zone, but attenuated to an uplift of about 4.5 cm of the ground surface.

Evolution of stress perturbations within the reservoir can be conveniently analyzed by plotting the stress path diagrams using the Mohr-Coulomb criterion for the characteristic locations in the model (Fig. 14).

The Mohr-Coulomb criterion is the most common failure criterion encountered in rock engineering. Many geomechanical analysis methods and programs require the use of this strength model. The Mohr-Coulomb criterion describes a linear relationship between normal and shear stresses (or maximum and minimum principal stresses) at failure.

The direct shear formulation of the criterion is given by

$$\tau = C + \sigma_n \tan \varphi \quad (3)$$

Where C is the cohesive strength and φ is the friction angle.

For the reservoir rock, the stress path diagrams show an increase of both the normal effective stress and the shear stress for depletion and an equally large decrease of both stresses for injection (at scenario 4 the maximum principal stress direction has been reversed). Also according to the Mohr-Coulomb criterion envelope, only at CO₂ injection pressure of 11,000 Psi, instability will occur in the reservoir (Fig. 14). Though, in other three scenarios the stress paths do not show a critical behavior, i.e., the paths is not converging towards the Mohr-Coulomb failure envelopes plotted for the shear strength parameters. It is noted that in these three scenarios deformation is elastic and the reservoir stress path for injection is fully reversible with reference to the stress path for depletion.

5. Conclusions

The relation between stresses, strains and fluid flow is complicated but solving it is the key to knowing the field stress state and its subsidence/uplift over the years. The flow will alter the stress and the porosity-permeability; as the result, the coupling in reservoir simulator and geomechanics is necessary and also very popular nowadays. In this paper a geomechanical reservoir modeling tool is established utilizing the ABAQUS scripting interface. The link consists of a set of FORTRAN code that rebuilds the ECLIPSE reservoir geometry and history in ABAQUS/CAE and vice-versa to evaluate the hydro-mechanical assessment for a given production or injection site. For the given parameters and the four considered scenarios the following finding were noted:

- At the start, each well production rate is 3,500 stb/day. Due to reservoir pressure reduction, the oil production rate will be decreased gradually. The production rate of well No.1 falls under 500 stb/day after about 3410 days from the start of production, so its production will be halted and it will be prepared for CO₂ injection. Injection strategy involves the injection of 200

mmscf/day and four scenarios for the maximum bottom hole pressure equal to 5000, 7000, 9000 and 11000 Psi.

- The production wells termination times and the termination reason (low production rate or $GOR > 20$ mscf/stb) depend on the value of CO_2 injection pressure.
- In the case of lower maximum bottom hole injection pressure, the cumulative oil production is more than other scenarios. Moreover at the high injection pressures, the production rates will not change with the injection bottom hole pressure variations. So in this reservoir, CO_2 injection with a maximum bottom hole pressure of 5000 Psi is suggested to increase oil production.
- Since lifetime of the reservoir in scenario 1 is greater than scenarios 2 and 3, the cumulative injection of carbon dioxide in scenario 1 is also more than the other two scenarios. However, in scenario 4 because of more bottom-hole pressure, the cumulative CO_2 injection is more than three other scenarios.
- The pressure is maximum in the injection zone with a distance inferior to 100 m from the injection wellbore. This zone can be considered as the most critical part of the system. Beside this distance, the pressure decreases significantly.
- As soon as CO_2 injection starts, changes in reservoir stress and strain can quickly propagate laterally within the injection zone, along with an expanding fluid pressure. The pressurization causes vertical expansion of the reservoir and changes in the stress field. These induced changes are, in general, proportional to the magnitude of the pressure increase, ΔP , and depend on the geometry and geomechanical properties of the reservoir and surrounding medium.
- The uplift is somewhat restricted by the overburden stiffness; the vertical displacement is about 6 cm at the top of the injection zone, but attenuated to an uplift of about 4.5 cm of the ground surface.
- The finite element analysis of the reservoir showed no sign of plastic strain under production and gas injection phases of scenarios 1, 2 and 3 in any part of the reservoir but in scenario 4 (11000 Psi) plastic strain has occurred in some parts of the reservoir like the anticline part and side burdens and the related stresses path show a critical behavior.
- Unlike scenario 4, in other three scenarios the stress paths do not show a critical behavior. In these three scenarios deformation is elastic and the reservoir stress path for injection is fully reversible with reference to the stress path for depletion.

References

- ABAQUS Unified Finite Element Analysis (2010), User's Manual Version 6.10, Providence, Rhode Island, Dassault Systèmes, Simulia Corporation, USA.
- Alavi, M. (2004), "Regional stratigraphy of the Zagros fold-thrust belt of Iran and its proforeland evolution", *Am. J. Sci.*, **304**, 1-20.
- Alavian, S.A and Whitson, C. (2009), "Modeling CO_2 Injection in a Fractured Chalk Experiment", *SPE 125362*, presented at the *SPE/EAGE Reservoir Characterization and Simulation Conference held in Abu Dhabi*, UAE, October.
- Bauer, S., Class, H., Ebert, M., Feeser, V., Götze, H., Holzheid, A., Kolditz, O., Rosenbaum, S., Rabbel, W., Schäfer, D. and Dahmke, A. (2012), "Modeling, parameterization and evaluation of monitoring methods for CO_2 storage in deep saline formations: the CO_2 -MoPa project", *Environ. Earth Sci.*, **67**, 351-367.
- Bielinski, A. (2007), "Numerical simulation of CO_2 sequestration in geological formations", Universität Stuttgart, Mitteilungsheft.

- Biot, M.A. (1940), "General theory of three-dimensional consolidation", *J. Appl. Phys.*, **12**, 155-164.
- Blunt, M., Fayers, F.J and Orr, F.M. (1993), "Carbon dioxide in enhanced oil recovery", *Energy Convers. Manage.*, **34**(9-11), 1197-1204.
- Carneiro, J.F. (2009), "Numerical simulations on the influence of matrix diffusion to carbon sequestration in double porosity fissured aquifers", *Int. J. Greenhouse Gas Control*, **3**(4), 431-443.
- Chales, P.A. and Roatesi, S. (1999), "A fully analytical solution of wellbore stability problem under undrained condition using a linearised Cam-Clay model", *Oil Gas Sci. Tech.*, **54**(5), 551-563.
- Dean, R.H., Gai, X., Stone, C.M and Minkoff, S.E. (2003), "A comparison of techniques for coupling porous flow and geomechanics", *Proceedings of the 17th SPE reservoir simulation symposium*, SPE 79709.
- Dusseault, M.B. (2011), "Geomechanical challenges in petroleum reservoir exploitation", *KSCE J. Civil Eng.*, **15**(4), 669-678.
- ECLIPSE Reservoir Simulation Software (2010), Version 2010 User Guide, Schlumberger.
- Eigestad, G.T., Dahle, H.K., Hellevang, B., Riis, F., Johansen, T. and Qian, E. (2009), "Geological modeling and simulation of CO₂ injection in the Johansen formation", *Comput. Geosci.*, **13**(4), 435-450.
- Elyasi, A., Goshtasbi, K., Saeidi, O. and Torabi, S.R. (2014). "Stress determination and geomechanical stability analysis of an oil well of Iran", *Sadhana*, **39**(1), 207-220.
- Elyasi, A. and Goshtasbi, K. (2015), "Using different rock failure criteria in wellbore stability analysis", *Geomech. Energy Environ.*, **2**, 15-21.
- Ferguson, R.C., Kuuskraa, V.A., Leeuwen, T.S.V. and Remson, D. (2010), "Storing CO₂ with Next-Generation CO₂-EOR Technology", *SPE 139717, presented at the SPE International Conference on CO₂ Capture, Storage, and Utilization*, New Orleans, Louisiana, USA, November.
- Fjaer, E. (1992), *Petroleum Related Rock Mechanics*, Elsevier Publications.
- Goshtasbi, K., Elyasi, A. and Naeimipour, A. (2014), "Stability assessment of a dual-opposing well junction", *Petrol. Sci. Tech.*, **32**(7), 790-796.
- Hayek, M., Mouche, E. and Mügler, C. (2009), "Modeling vertical stratification of CO₂ injected into a deep layered aquifer", *Adv. Water Resour.*, **32**(3), 450-462.
- Holt, T., Jensen, J.I. and Lindeberg, E. (1995), "Underground storage of CO₂ in aquifers and oil reservoirs", *Energy Convers. Manage.*, **36**(6-9), 535-538.
- Holt, T., Lindeberg, E. and Taber, J. (2000), "Technologies and possibilities for larger-scale CO₂ separation and underground storage", *SPE 63103, presented at the SPE Annual Technical Conference and Exhibition*, Dallas, Texas, USA, October.
- Izgec, O., Demiral, B., Bertin, H.J. and Akin, S. (2005), "Experimental and numerical investigation of carbon sequestration in saline aquifers", *SPE 94697, presented at the SPE/EPA/DOE Exploration and Production Environmental Conference*, Galveston, Texas, USA, March.
- Jahangiri, H.R. and Zhang, D. (2010), "Optimization of carbon dioxide sequestration and enhanced oil recovery in oil reservoir", *SPE 133594, presented at the SPE Western Regional Meeting*, Anaheim, California, USA, May.
- Kaarstad, E. and Aadnoy, B.S. (2005), "Optimization of borehole stability using 3D stress optimization", *SPE Annual Technical Conference and Exhibition*, Texas, Dallas, SPE-97149-MS.
- Kumar, A., Noh, M., Pope, G.A., Sepehrnoori, K., Bryant, S. and Lake, L.W. (2004), "Reservoir simulation of CO₂ storage in deep saline aquifers", *SPE 89343, presented at the SPE/DOE Symposium on Improved Oil Recovery*, Tulsa, Oklahoma, USA, April.
- Lerat, O., Adjemian, F., Auvinet, A., Baroni, A., Bemmer, E., Eschard, R., Etienne, G., Renard, G., Servant, G., Michel, L., Rodriguez, S., Aubin, F. and Euzen, T. (2009), "Modelling of 4D Seismic Data for the Monitoring of the Steam Chamber Growth during SAGD Process", *Proc., Canadian International Petroleum Conference 2009*, Calgary, Alberta, Canada, June.
- Liu, X., Gong, B. and Huo, D. (2010), "Numerical Simulation on CO₂ Sequestration in Saline Formations With Natural or Hydraulic Fractures Using a Discrete Modeling Approach", *SPE 137621, presented at the Canadian Unconventional Resources and International Petroleum Conference*, Alberta, Canada, October.
- Martin, D. and Taber, J. (1992), "Carbon dioxide flooding", *J. Petrol. Tech.*, **44**(4), 396-400.
- Todd, M. and Grand, G. (1993), "Enhanced oil recovery using carbon dioxide", *Energy Convers. Manage.*,

- 34(9-11), 1157-1164.
- Metz, B. (2005), *IPCC special report on carbon dioxide capture and storage*, Cambridge University Press.
- Jessen, K., Kovscek, A.R. and Orr, F.M. (2005), "Increasing CO₂ storage in oil recovery", *Energy Convers. Manage.*, **46**(2), 293-311.
- Moortgat, J., Firoozabadi, A., Li, Z. and Esposito, R. (2010), "A detailed experimental and numerical study of gravitational effects on CO₂ enhanced recovery", *SPE 135563, presented at the SPE Annual Technical Conference and Exhibition*, Florence, Italy, September.
- Nasrabadi, H., Firoozabadi, A. and Ahmed, T. (2009), "Complex flow and composition path in CO₂ injection schemes from density effects in 2 and 3D", *SPE 124803, presented at the SPE Annual Technical Conference and Exhibition*, New Orleans, Louisiana, USA, October.
- Nghiem, L., Shrivastava, V., Kohse, B., Hassam, M. and Yang, C. (2010), "Simulation and optimization of trapping processes for CO₂ storage in saline aquifers", *J. Can. Petrol. Tech.*, **49**(8), 15-22.
- Oldenburg, C., Pruess, K. and Benson, S.M. (2001), "Process modeling of CO₂ injection into natural gas reservoirs for carbon sequestration and enhanced gas recovery", *Energy Fuel.*, **15**(2), 293-298.
- Park, Y.C., Huh, D.G. and Park, C.H. (2012), "A pressure-monitoring method to warn CO₂ leakage in geological storage sites", *Environ. Earth Sci.*, **67**, 425-433.
- Ravagnani, A.G., Ligerio, E. and Suslick, S. (2009), "CO₂ sequestration through enhanced oil recovery in a mature oil field", *J. Petrol. Sci. Eng.*, **65**(3-4), 129-138.
- Rutqvist, J., Wu, Y.S., Tsang, C.F. and Bodvarsson, G. (2002), "A modeling approach for analysis of coupled multiphase fluid flow, heat transfer, and deformation in fractured porous rock", *Int. J. Rock Mech. Min. Sci.*, **39**, 429-442.
- Sbai, M. and Azaroual, M. (2010), "Numerical modeling of formation damage by two-phase particulate transport processes during CO₂ injection in deep heterogeneous porous media", *Adv. Water Resour.*, **34**, 62-82.
- Settari, A. and Mourits, F.M. (1998), "A coupled reservoir and geomechanical simulation system", *SPE J.*, **3**, 219-226.
- Settari, A. and Walters, D. (1999), "Advances in coupled geomechanical and reservoir modeling with applications to reservoir compaction", *Proceedings of SPE Reservoir Simulation Symposium, Society of Petroleum Engineers*, Houston, Texas.
- Shi, J.Q. and Durucan, S. (2009), "A coupled reservoir-geomechanical simulation study of CO₂ storage in a nearly depleted natural gas reservoir", *Energy Procedia*, **1**, 3039-3046.
- Sifuentes, W., Giddins, M. and Blunt, M. (2009), "Modeling CO₂ Storage in Aquifers: Assessing the key contributors to uncertainty", *SPE 123582, presented at the Offshore Europe*, Aberdeen, UK, September.
- Sun, S. and Firoozabadi, A. (2009), "Compositional modeling in three-phase flow for CO₂ and other fluid injections using higher-order finite element methods", *SPE 124907, presented at the SPE Annual Technical Conference and Exhibition*, New Orleans, Louisiana, USA, October.
- Thomas, L.K., Chin, L.Y., Pierson, R.G. and Sylte, J.E. (2003), "Coupled Geomechanics and Reservoir Simulation", *SPE J.*, **8**, 350-358.
- Thomas, S. and Wheeler, M. (2011), "Multiblock methods for coupled flow-transport and compositional flow through porous media-Applications to the simulation of transport of reactive species and carbon sequestration", *SPE 141824, presented at the SPE Reservoir Simulation Symposium*, Woodlands, Texas, USA, February.
- Touhidi-Baghini, A. (1998), "Absolute permeability of McMurray formation oil sands at low confining stresses", PhD Dissertation, Department of Civil Engineering, University of Alberta, Alberta.
- Vidal-Gilbert, S., Nauroy, J.F. and Brosse, E. (2009), "3D geomechanical modelling for CO₂ geologic storage in the Dogger carbonates of the Paris Basin", *Int. J. Greenhouse Gas Control*, **3**, 288-299.
- Zandi, S., Renard, G., Nauroy, J.F., Guy, N. and Tijani, M. (2010), "Numerical modelling of geomechanical effects during steam injection in SAGD heavy oil recovery", *Paper SPE 129250 presented at the EOR Conference at Oil & Gas West Asia*, Muscat, Oman, April.
- Zhou, S., Hillis, R. and Sandiford, S. (1996), "On the mechanical stability of inclined wellbore", *SPE Drill. Complet.*, **2**, 67-73.

Zienkiewicz, O.C., Chan, A.H.C., Pastor, M., Schrefler, B.A. and Shiomi, T. (1999), *Computational Geomechanics with Special Reference to Earthquake Engineering*, John Wiley and Sons.

CC